Available online at www.sciencedirect.com
SCIENCE DIRECT®
Journal of Power Sources 125 (2004) 292–298
JOURNAL OF POWER SOURCES
www.elsevier.com/locate/jpowsour

Electrochemical characterization of activated carbon–ruthenium oxide nanoparticles composites for supercapacitors

Wei-Chun Chen [a], Chi-Chang Hu [a,*], Chen-Ching Wang [a], Chun-Kuo Min [b]

[a] *Department of Chemical Engineering, National Chung Cheng University, Chia-Yi 621, Taiwan*
[b] *Union Chemical Laboratories, Industrial Technology Research Institute, Hsinchu 310, Taiwan*

Received 23 April 2003; received in revised form 4 August 2003; accepted 6 August 2003

Abstract

The high specific capacitance of ruthenium oxide (denoted as RuO_x) nanoparticles prepared by a modified sol–gel method with annealing in air for supercapacitors was demonstrated in this work. The specific capacitance of activated carbon (denoted as AC) measured at 5 mA/cm^2 is significantly increased from 26.8 to 38.7 F/g by the adsorption of RuO_x nanoparticles with ultrasonic weltering in 1 M NaOH for 30 min. This method is a promising tool in improving the performance of carbon-based double-layer capacitors. The total specific capacitance of a composite composed of 90 wt.% AC and 10 wt.% RuO_x measured at 25 mV/s is about 62.8 F/g, which is increased up to ca. 111.7 F/g when RuO_x has been previously annealed in air at 200 °C for 2 h. The specific capacitance of RuO_x nanoparticles was promoted from 470 to 980 F/g by annealing in air at 200 °C for 2 h. The nanostructure of RuO_x was examined from the transmission electron microscopic (TEM) morphology.

Keywords: Composites; RuO_x nanoparticles; Activated carbon; Supercapacitors

1. Introduction

Supercapacitors, delivering electric energy in the pulse form, usually consist of highly porous materials (e.g., activated carbon) with a high specific surface area [1,2]. These devices are also called double-layer capacitors because charges are stored within the electric double layers at the electrode–electrolyte interface. On the other hand, the electrochemical supercapacitors employing electroactive materials to store the electric energy through means of Faradaic reactions are generally called pseudocapacitors [3–5]. In addition, the Faradaic redox reactions within these electroactive materials have to be highly reversible in order to exhibit the high power merit of supercapacitors [1–5]. Therefore, the performance of electrochemical supercapacitors is usually determined by the electrochemical characteristics of electroactive materials.

Ruthenium oxides prepared by several methods have been widely recognized as promising materials for electrochemical supercapacitors due to their high specific capacitance [1–3,6–8]. The specific capacitance of amorphous Ru oxide prepared by a sol–gel method has been reported to reach 760 F/g [6,7]. However, due to the high cost of ruthenium precursor, their practical usage is limited. Accordingly, several studies investigate the capacitive performance of activated carbon–ruthenium oxide composites [9–14]. In these studies, the total specific capacitance of composites is a function of the Ru oxide content since Ru oxide is the main electroactive material providing the Faradaic pseudocapacitance. In addition, the specific capacitance of Ru oxide can be enhanced by annealing in air at temperatures $\leq$150 °C [4,6,7,10], by electrochemical anodizing in aqueous media [15], or by ultrasonic weltering in NaOH [16]. Although the specific capacitance of Ru oxide in these studies is high, the reproducibility for obtaining the high specific capacitance of Ru oxide is not good in our recent tests.

Based on the above viewpoints, a relatively simple process for fabricating hydrous ruthenium oxide with its specific capacitance $\geq$700 F/g is developed in this work. In addition, the electrochemical characteristics of composite electrodes composed of AC powders and the hydrous RuO_x nanoparticles prepared by a modified sol–gel method are investigated for the application of supercapacitors. The effects of annealing in air for ruthenium oxide nanoparticles on the capacitive performance of AC–RuO_x composites are also studied in this work, since annealing has been proposed to be

* Corresponding author. Tel.: +886-5-272-0411x33411; fax: +886-5-272-1206.
E-mail address: chmhcc@ccu.edu.tw (C.-C. Hu).

0378-7753/$ – see front matter © 2003 Elsevier B.V. All rights reserved.
doi:10.1016/j.jpowsour.2003.08.001

a key factor promoting the specific capacitance of Ru oxide [7,12]. For a practical purpose, all current collectors used in this work are stainless steel (SS-316) meshes since the utilization of electrode materials on a mesh-type substrate is better than that on a plate-type current collector [16].

2. Experimental

An aqueous solution consisting of 50 mM $RuCl_3 \cdot xH_2O$ was well stirred at room temperature for 20 min and methanol of the same volume was added into the stirred solution for 20 min in order to form the organometallic species. After stirring, a 1 M NaOH solution was slowly dropped into this precursor solution until pH reaches 7.0 and this solution was agitated at room temperature for 1 h. Ruthenium precipitates were clearly found after sedimentation (i.e., hydrolysis, condensation, and polymerization simultaneously occurred to form the ruthenium precipitates by the addition of NaOH). The precipitates were repeatedly shaken with pure water for 20 min ($\geq$4 times) to remove the residual chloride ($[Cl^-] < 10^{-5}$ M). Finally, the cleaned precipitates were dissolved in an aqueous NH_3 solution and shaken at 200 rpm in a water bath at 60 °C for 2 h to form a meta-stable hydrous ruthenium oxide colloid solution (i.e., reconstructing the Ru oxide nanoparticles). For a conventional sol–gel process, alkoxides are usually prepared from a reflux process in alcohol solutions for a long time (e.g., at 120 °C for 24 h) and then, hydrolysis of the alkoxides results in the formation of hydroxides. A condensation reaction occurs between these hydroxides to form dimmers and/or oxide clusters and finally, oxides in various structures are formed from a polymerization step. Thus, the procedure and steps in the modified process are more simple and moderate in comparison with the conventional one, which should be more practically useful.

Stainless steel meshes were cleaned before the application of AC or AC–RuO_x coatings. These 10 mm × 10 mm substrates were first etched in an ultrasonic HCl solution (0.1 M) at room temperature for 5 min and then, degreased with pure water and dried in a vacuum oven at room temperature overnight. Activated carbon powders were ground from AC particles with a specific surface area of 750 m^2/g and mean pore size of 18 Å.

There were two procedures for the preparation of AC–RuO_x composite electrodes in this work. In the first procedure, AC powders were dispersed in the meta-stable Ru oxide colloid solution with ultrasonic vibration for 2 h. These powders were filtered and dried in a vacuum oven at room temperature overnight. These dried powders were mechanically mixed with the polyvinylidene difluoride (PVdF) binder of 5 wt.% for 30 min and then, methyl-2-pyrrolidone was dropped into the mixture and ground to form sticky coating slurry. This slurry was smeared onto the cleaned SS mesh and then, dried in a vacuum oven at 85 °C for 8 h (denoted as AC-adsorbed RuO_x/SS). Some electrodes were subjected to the ultrasonic weltering in 1 M NaOH for 30 min. These pretreated electrodes were ultrasonic cleaned in pure water for 5 min before capacitive measurements. Note that all AC-adsorbed RuO_x/SS electrodes were never annealed in air. In the second procedure, AC and RuO_x powders in specified weight ratios were well mixed with the 5 wt.% PVdF powders for 30 min. The solvent was dropped into the above mixture and ground to form the coating slurry. This slurry is smeared onto the pretreated SS mesh and then dried in a vacuum oven at 85 °C for 8 h (denoted as AC–RuO_x/SS). Note that some RuO_x powders were annealed in air under specified conditions before mechanically mixed with AC powders to investigate the effects of annealing in air for RuO_x nanoparticles on the capacitive performance of AC–RuO_x/SS electrodes. In addition, all AC–RuO_x/SS electrodes were not ultrasonically weltered in NaOH.

The electrochemical measurements were performed through means of an electrochemical analyzer system, CHI 633A (CH Instruments, USA). All experiments were carried out in a three-compartment cell. An Ag/AgCl electrode (Argenthal, 3 M KCl, 0.207 V versus SHE at 25 °C) was used as the reference and a piece of platinum gauze with an exposed area equal to 4 cm^2 was employed as the counter electrode. A Luggin capillary, whose tip was set at a distance of 1–2 mm from the surface of the working electrode, was used to minimize errors due to *iR* drop in the electrolytes. The nanostructure of ruthenium oxide was examined by means of a transmission electron microscope (TEM, Hitachi, H-7100).

All solutions used in this work were prepared with 18 MΩ cm water produced by a reagent water system (Milli-Q SP, Japan). $RuCl_3 \cdot xH_2O$ used in this work is from Alfa Aesar (USA). The electrolytes used for the capacitive characterization of composite electrodes were degassed with purified nitrogen gas before measurements for 25 min and this nitrogen was passed over the solutions during the measurements. The solution temperature was maintained at 25 °C by means of a water thermostat (Haake DC3 and K20).

3. Results and discussion

3.1. TEM morphologies of RuO_x prepared by the modified sol–gel method

The size of RuO_x particles prepared by means of the modified sol–gel method was estimated from the TEM photographs. Typical results are shown in Fig. 1a and b at the magnification of 120,000. In Fig. 1a, the particle size of RuO_x aggregates ranges from ca. 30 to 60 nm, while these particles are believed to be aggregates of many small RuO_x clusters. This statement is further supported by the fact that many RuO_x precipitates became visible if this solution was kept in a bottle for about 12 h at room temperature (i.e., a

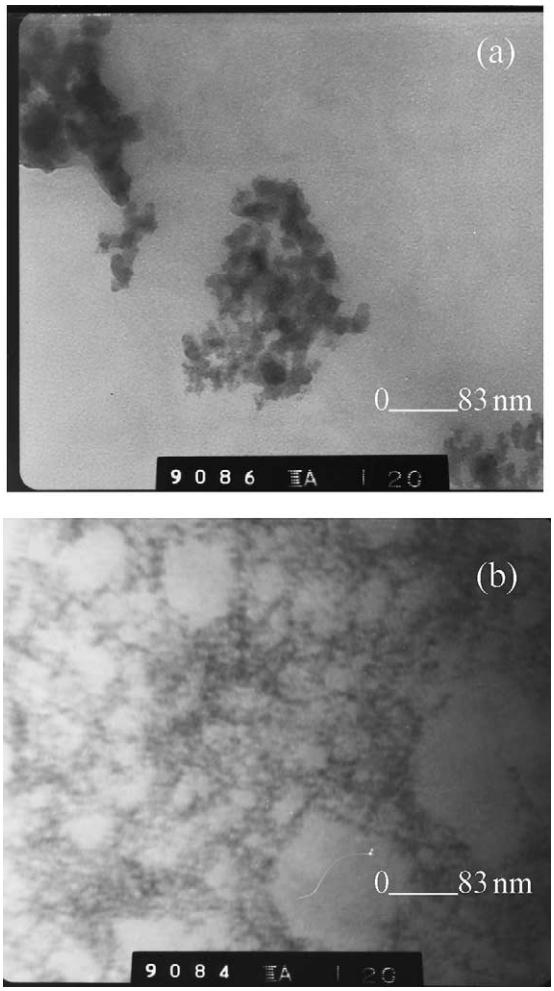

Fig. 1. TEM photographs under the magnification of 120,000× for (a) as-prepared RuO_x nanoparticles prepared by a modified sol–gel method and (b) those with an ultrasonic vibration for 15 min.

meta-stable RuO_x colloid solution). These precipitates can be re-dispersed into the solution when this solution was vibrated in an ultrasonic bath for 5 min. In Fig. 1b, RuO_x in the nano-network structure is clearly found, which was prepared from the meta-stable RuO_x colloid solution with the ultrasonic vibration for 15 min. The formation of this nano-network structure should be favored by the presence of well-dispersed Ru clusters, which further supports that RuO_x nanoparticles should be the aggregates consisting of many small RuO_x clusters.

3.2. Capacitive performance of AC-adsorbed RuO_x composites

Curves 1–3 shown in Fig. 2 represent the voltammetric responses of an AC/SS electrode, an AC-adsorbed RuO_x/SS electrode, and the AC-adsorbed RuO_x/SS electrode with ultrasonic weltering in 1 M NaOH for 30 min, respectively. On curve 1, the AC/SS electrode shows the capacitive-like responses in the potential window of investigation. However,

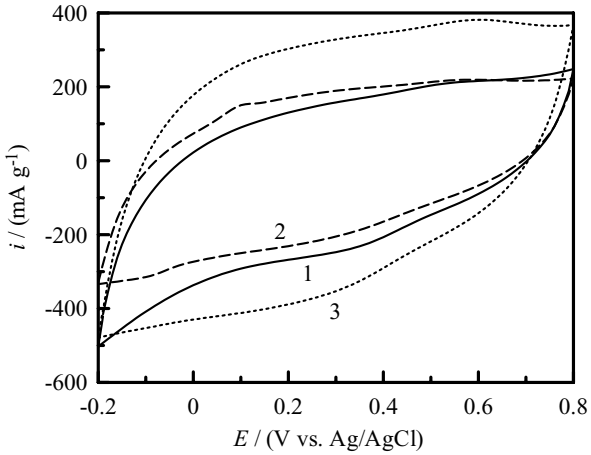

Fig. 2. Cyclic voltammograms of (1) an AC/SS electrode with the specific surface area of AC = 750 m^2/g; (2) an AC-adsorbed RuO_x/SS electrode; and (3) an AC-adsorbed RuO_x/SS electrode with ultrasonic weltering in 1 M NaOH for 30 min. CV curves were measured at 10 mV/s in 0.1 M H_2SO_4.

there exists a rise in voltammetric currents with the positive shift in electrode potentials on both positive and negative sweeps, especially at a relatively rapid scan rate. This result is indicative of the significant resistance on this electrode, which is attributable to a combination of: (i) the contact resistance at the interface between AC and the current collector and (ii) the diffusion barrier of hydrated ions within the micropores of AC. Note that the specific capacitance of an AC/SS electrode (based on the weight of activated carbon) is only 20 F/g at 10 mV/s, which is much lower than the theoretic value estimated from the specific surface area of AC (i.e., 750 m^2/g × 10,000 cm^2/m^2 × 15 × 10^{-6} F/g = 112.5 F/g). This phenomenon is due to the obscuration of the mesopores and micropores with the PVdF binders since the specific surface area of AC with PVdF binders determined by the BET method is only close to 300 m^2/g. From a comparison of curves 1 and 2, better capacitive-like responses are found on the AC-adsorbed RuO_x/SS electrode while the charges surrounded in curve 2 are not increased by the adsorption of few RuO_x nanoparticles. However, the contribution of these RuO_x nanoparticles adsorbed into the AC powders can be enhanced when this AC-adsorbed RuO_x electrode has been weltered in an ultrasonic bath of 1 M NaOH (see curve 3). Thus, the capacitive characteristics of AC can be improved by a combination of the adsorption of minor RuO_x nanoparticles and the ultrasonic weltering in NaOH since an AC/SS electrode with the same treatment does not show the similar improved phenomenon. Moreover, the total specific capacitance of this electrode increases to ca. 27.5 F/g when the scan rate of CV is equal to 10 mV/s. This result indicates that the specific capacitance of RuO_x nanoparticles with the ultrasonic weltering in NaOH should be very high since the content of adsorbed RuO_x nanoparticles within this composite is too small to be precisely determined.

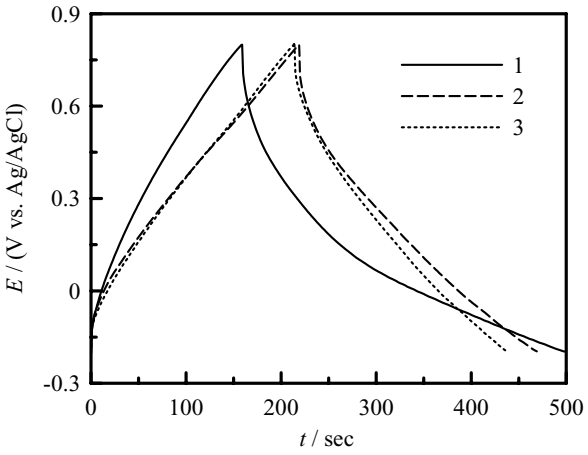

Fig. 3. Chronopotentiograms of (1) an AC/SS electrode; (2) an AC-adsorbed RuO_x/SS electrode; and (3) an AC-adsorbed RuO_x/SS electrode with ultrasonic weltering in 1 M NaOH for 30 min. CPs were measured at 5 mA/cm^2 in 0.1 M H_2SO_4.

Chronopotentiomograms of an AC/SS electrode, an AC-adsorbed RuO_x/SS electrode, and the AC-adsorbed RuO_x/SS electrode with ultrasonic weltering in NaOH measured in 0.1 M H_2SO_4 at 5 mA/cm^2 are shown as curves 1–3 in Fig. 3, respectively. Note that on curve 1, the *iR* drop is about 90 mV as the current polarity is altered, indicating that the overall resistance of the AC/SS electrode is about 9 Ω. In addition, the charge curve is not symmetric to its discharge counterpart. The specific capacitance of AC measured at 5 mA/cm^2 is about 26.8 F/g in the charge process while there is an irreversible reduction occurs at ca. 0.1 V in the discharge process. The former result indicates that the specific capacitance of AC is strongly dependent upon the scan rates of CV or the current density of chronopotentiometry. This information suggests that micropores provide a large portion of surface areas for the employed AC powders, resulting in the incomplete structure of the electric double layers within them. In addition, the micropores within AC should be tortuous, increasing the movement barrier of hydrated ions. All the above results suggest the relatively poor capacitive characteristics of bare activated carbon. On curve 2, the charge curve of an AC-adsorbed RuO_x composite is symmetric to its discharge counterpart. This ideally capacitive performance is also clearly found on curve 3. Hence, the capacitive performance of AC can be significantly improved by the adsorption of RuO_x nanoparticles. Also, note that the specific capacitance obtained from curves 2 and 3 is 30.2 and 38.7 F/g, respectively. Therefore, the capacitive characteristics of the AC-adsorbed RuO_x electrode with ultrasonic weltering in NaOH is much better than that of AC/SS or the pristine AC-adsorbed RuO_x electrodes. Since the loading of AC-adsorbed RuO_x composites on the above two electrodes is different, the similar charge–discharge periods for curves 2 and 3 in Fig. 3 are not indicative of the similar specific capacitance for an AC-adsorbed RuO_x/SS electrode and the AC-adsorbed RuO_x/SS electrode with ultrasonic weltering in NaOH. Based on all the above results and discussion, the double-layer capacitive characteristics of AC can be significantly improved by a combination of the adsorption of RuO_x nanoparticles and the ultrasonic weltering in NaOH.

3.3. Capacitive performance of AC–RuO_x composites

Based on the cost consideration, composites composed of AC powders and RuO_x nanoparticles (denoted as AC–RuO_x) with acceptable capacitive characteristics should be a suitable electrode material for the supercapacitor application. Curves 1 and 2 in Fig. 4 show the voltammetric behavior measured in 0.1 M H_2SO_4 at 25 mV/s for an AC/SS electrode and an AC–RuO_x/SS composite with 10 wt.% of RuO_x nanoparticles. From a comparison of curves 1 and 2, Faradaic currents due to the redox transition of RuO_x nanoparticles are clearly found on both positive and negative sweeps of curve 2. In addition, two broad peaks with their peak potentials at ca. 0.6 and 0.3 V are clearly observed on the positive and negative sweeps of curve 2, respectively. In fact, this composite shows the capacitive responses similar to a thick $RuO_x{\cdot}nH_2O$-coated Ti electrode prepared by the CV deposition [8]. Based on the above results and discussion, the increase in voltammetric current density of this AC–RuO_x composite must be due to the redox transitions of RuO_x nanoparticles. Unfortunately, there still exists a rise in currents with the positive shift in electrode potentials on both positive and negative sweeps of curve 2 in Fig. 4, indicative of the significant resistance on this AC–RuO_x/SS electrode. There are probably two reasons responsible for the above phenomenon for this AC–RuO_x composite. First, the electrochemical characteristics of RuO_x nanoparticles prepared by the modified sol–gel method are likely not as good as those reported in the literature [9–14]. This statement is supported by the result that an AC-adsorbed RuO_x composite has to be activated by the ultrasonic weltering

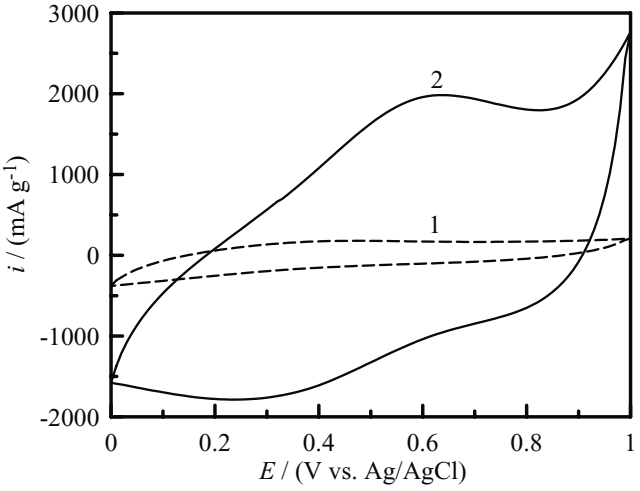

Fig. 4. Cyclic voltammograms of (1) AC/SS and (2) AC–RuO_x/SS electrodes with 10 wt.% of RuO_x nanoparticles. CV curves were measured at 25 mV/s in 0.1 M H_2SO_4.

in NaOH (see Fig. 2). Second, the significant contact resistance between electrode materials and the current collector should result from the poor adhesion between the AC–RuO_x composite and SS mesh because composites are only mechanically smeared onto the current collector. If this is the case, the large contact resistance between AC–RuO_x and SS should increase the barrier of electron hopping between electrode materials and current collectors.

The specific capacitance of the AC–RuO_x composite can be calculated on the basis of the following formula [3,15,17]:

$$C_{S,T} = \frac{q^*}{w\Delta V} \quad (1)$$

where $C_{S,T}$, q^*, w, and ΔV represent the total specific capacitance of AC–RuO_x, the average of anodic and cathodic charges integrated from the positive and the negative sweep of CV, loading of the composite, and the potential window of CV. The specific capacitance of this AC–RuO_x composite measured at 25 mV/s is about 62.8 F/g. The specific capacitance of RuO_x nanoparticles can be estimated from the following equation [15,16]:

$$C_{S,\mathrm{Ru}} = \frac{C_{S,T} - (1 - w_{\mathrm{Ru}})C_{S,C}}{w_{\mathrm{Ru}}} \quad (2)$$

where $C_{S,\mathrm{Ru}}$, $C_{S,C}$, and w_{Ru} represent the specific capacitance of RuO_x, the specific capacitance of AC, and the weight fraction of RuO_x within the AC–RuO_x composite, respectively. The specific capacitance of these RuO_x nanoparticles is about 470 F/g.

From the results reported by Zheng and Jow [6,7], hydrous Ru oxide prepared by a sol–gel method exhibited a better electrochemical reversibility and higher specific capacitance when it has been annealed in air at a critical temperature close to the crystallization temperature. This phenomenon has been attributed to the local structures of AC–RuO_x composites retaining facile pathways for both electrons and protons [12,18]. Accordingly, RuO_x nanoparticles before mixed with AC powders were annealed in air at several temperatures (i.e., 100, 150, and 200 °C) in order to promote the utilization of the ruthenium species and to improve the capacitive characteristics of AC–RuO_x composites. Typical cyclic voltammograms measured in 0.1 M H_2SO_4 at 25 mV/s for the AC–RuO_x composites with RuO_x nanoparticles annealed at 100, 150, and 200 °C for 1 h are presented as curves 1, 3, and 5 in Fig. 5 meanwhile those annealed at 100, 150, and 200 °C for 2 h are shown as curves 2, 4 and 6, respectively, in the same figure. Note that all curves with the exception of curve 1 in Fig. 5 show higher voltammetric currents but similar capacitive behavior to the CV in Fig. 4. In addition, the lower potential limits of CV in Fig. 5 is −0.2 V, indicating a wider potential window for the charge storage in comparison with that in Fig. 4 since there is an irreversible reduction occurring at potential negative to −0.1 V for the AC–RuO_x composite without annealing. The above result reveals the fact that annealing in air can be used to improve the utilization and stability of RuO_x nanoparticles. Moreover, the improvement in capacitive performance of AC–RuO_x is not attributed to the interaction between RuO_x and AC because RuO_x nanoparticles were annealed in air before mixed with AC powders. It is worthy noting that the composite composed of AC and RuO_x annealed in air at 200 °C for 2 h shows the highest voltammetric current density as well as the best capacitive behavior from a comparison of curves 1–6 in Fig. 5. This temperature is obviously higher than 150 °C (proposed in the literature [6,7]). Moreover, in our previous work, hydrous ruthenium oxide deposited by cyclic voltammetry showed the crystalline peak at annealing temperatures ≥100 °C [19]. Based on these inconsistent results, the crystallization temperature of ruthenium oxides prepared by different methods is believed to be different. This difference in the crystallization temperature of ruthenium oxides should result from the differences in the mean oxidation state and/or the structure of their corresponding hydroxyl ruthenium species.

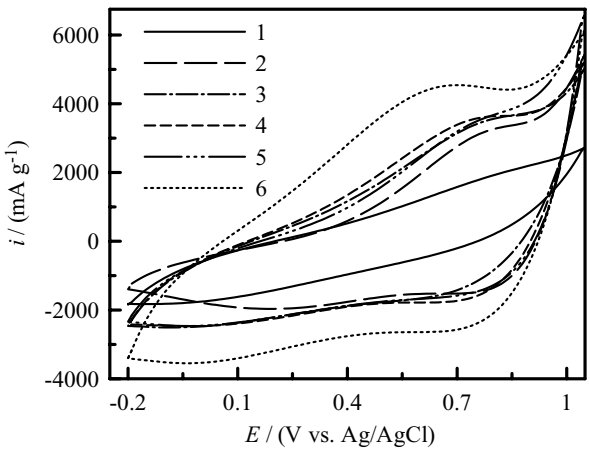

Fig. 5. Cyclic voltammograms of AC–RuO_x/SS electrodes with 10 wt.% of RuO_x measured at 25 mV/s in 0.1 M H_2SO_4. RuO_x nanoparticles were annealed in air at (1, 2) 100 °C; (3, 4) 150 °C and (5, 6) 200 °C for (1, 3, 5) 1 h and (2, 4, 6) 2 h.

Total specific capacitance of the AC–RuO_x composites shown in Fig. 5 and specific capacitance of their corresponding annealed RuO_x nanoparticles measured at 25 mV/s are shown in Table 1. With the exception of the composite composed of AC and RuO_x annealed at 100 °C for 1 h, the total specific capacitance of the other AC–RuO_x composites is significantly enhanced by the annealing treatment on RuO_x

Table 1
Total specific capacitances ($C_{S,T}$) of AC–RuO_x composites measured at 25 mV/s in 0.1 M H_2SO_4 and the corresponding specific capacitance of RuO_x nanoparticles ($C_{S,\mathrm{Ru}}$) with annealing in air at various conditions

	Sample					
	1	2	3	4	5	6
T_a (°C)	100	100	150	150	200	200
Time (h)	1	2	1	2	1	2
$C_{S,T}$ (F/g)	57.7	78.6	77.5	94.1	94.5	111.7
$C_{S,\mathrm{Ru}}$ (F/g)	420	630	620	780	790	980

meanwhile the composite composed of AC and RuO_x annealed in air at 200 °C for 2 h shows the highest total specific capacitance (111.7 F/g). The above results reveal the fact that annealing in air renders the better utilization of RuO_x and the wider potential window for the charge storage. In our opinion, the electronic conductivity of RuO_x nanoparticles may be poor because the amorphous nanostructure of RuO_x should result in the discontinuity of the electron pathway during the charge storage and delivery processes. However, this discontinuity in the electron pathways may be improved by the annealing treatment due to the sintering of RuO_x. If this is the case, there should be a synergistic effect for the composite composed of AC powders and annealed RuO_x, promoting the total specific capacitance of the resultant AC–RuO_x composites. Accordingly, a great promotion in the specific capacitance of RuO_x nanoparticles resulting from a higher utilization of Ru species is found. This statement is further supported by the fact that the specific capacitance of RuO_x nanoparticles, from all AC–RuO_x composites shown in Table 1, is ≥420 F/g on the basis of Eq. (2).

The effect of changing the upper potential limits of CV on the voltammetric behavior of an AC–RuO_x composite with 10 wt.% of annealed $RuO_x{\cdot}nH_2O$ nanoparticles (annealed at 200 °C for 2 h) are shown in Fig. 6. Note that this composite shows a fair reversibility in the 0.1 M H_2SO_4 solution at a scan rate of 25 mV/s. This result indicates that this composite is a potential candidate in the application of electrochemical supercapacitors. Since the scan rate of CV is moderate, the power property of this composite is high. However, the capacitive performance of this AC–RuO_x/SS electrode should be further improved by reducing the contact resistance between the AC–RuO_x composite and the SS current collector although the capacitive performance of this composite electrode is fairly satisfactory.

Typical chronopotentiograms measured in 0.1 M H_2SO_4 at 10, 5, 2, and 1 mA/cm^2 for another newly prepared AC–RuO_x composite with 10 wt.% of annealed $RuO_x{\cdot}nH_2O$ nanoparticles (annealed at 200 °C for 2 h) are shown as

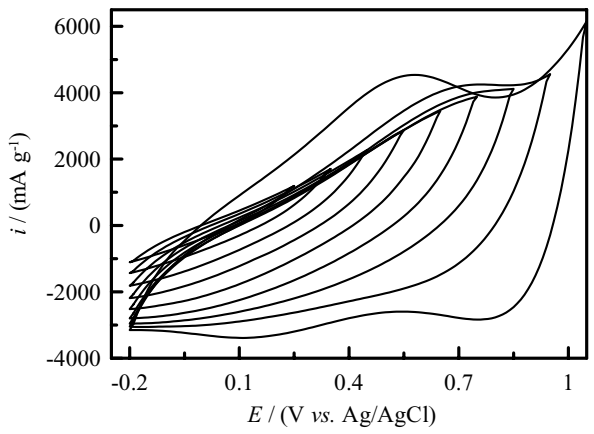

Fig. 6. Cyclic voltammograms of an AC–RuO_x/SS electrode with 10 wt.% of annealed RuO_x nanoparticles measured at 25 mV/s in 0.1 M H_2SO_4 with the negative shift in the upper potential limits of CV.

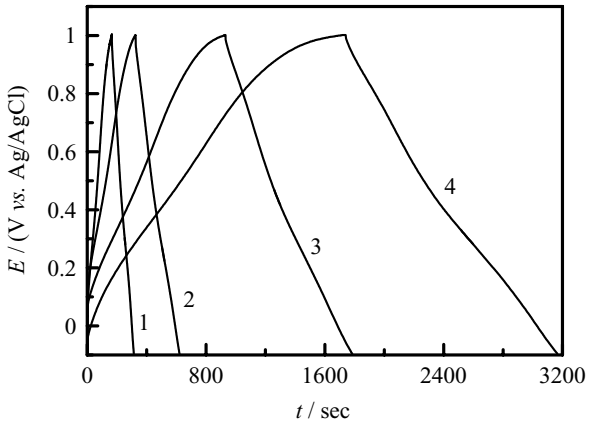

Fig. 7. Chronopotentiomograms of an AC–RuO_x/SS electrode with 10 wt.% of annealed RuO_x nanoparticles between −0.1 and 1.0 V at (1) 10.0 mA/cm^2; (2) 5.0 mA/cm^2; (3) 2.0 mA/cm^2; and (4) 1.0 mA/cm^2 in 0.1 M H_2SO_4.

curves 1–4 in Fig. 7, respectively. Note that the *iR* drops on curves 1 and 2 are much smaller than that shown in Fig. 3 when the applied currents are swept from anodic to cathodic, indicating the fact that the overall resistance of this AC–RuO_x/SS electrode is lower than that of an AC-adsorbed RuO_x/SS electrode. Moreover, the charge–discharge efficiency of the former electrode is also better than that of the later one. The above capacitive performance of this AC–RuO_x/SS electrode is also better than that of the AC–RuO_x composite with the RuO_x nanoparticles without annealing. All the above results indicate the better capacitive characteristics of an AC–RuO_x composite with annealed oxide. Unfortunately, there still exists an irreversible oxidation occurring at potentials positive than ca. 0.9 V in the charge process, especially under lower applied current densities (see curves 3 and 4 in Fig. 7). This result is attributed to the gradual dissolution of ruthenium species since RuO_4^{2-} is probably formed and dissolved in this potential region [20]. In fact, very dilute brown species attributable to a worse dissolution phenomenon are clearly found on an AC–RuO_x/SS electrode if the RuO_x nanoparticles have not been annealed. This dissolution phenomenon is approximately ceased as temperatures ≥150 °C for 2 h. Based on the above results and discussion, the most suitable potential window for an AC–RuO_x/SS electrode with RuO_x annealed in air at 200 °C for 2 h should be located between −0.2 and 0.9 V.

In our recent tests, it is very hard to obtain the high specific capacitance of Ru oxide (i.e., 760 F/g) prepared by the procedure described by Zheng et al. [6,7]. In addition, the crystalline temperatures of Ru oxides prepared in different laboratories are different [6,7,19] meanwhile the crystalline temperature was found to influence the specific capacitance of Ru oxide strongly. With these results and opinions in mind, the reproducibility for obtaining the high specific capacitance of Ru oxide is important for practical usage. Note that all the results shown in this work have been repeated and the specific capacitance of RuO_x annealed

in air at 200 °C ranged from 920 to 980 F/g after several repeats. In addition, the techniques in preparing the RuO_x nanoparticles, AC-adsorbed RuO_x/SS, and AC–RuO_x/SS electrodes were jointly developed and mutually checked by the Union Chemical Laboratories in the Industrial Technology Research Institute of Taiwan, revealing their promising application potential.

4. Conclusions

Ruthenium oxide nanoparticles with particle sizes from ca. 30 to 60 nm were successfully prepared by a modified sol–gel method. These particles were considered as aggregates composed of many small RuO_x clusters ($\leq$10 nm). A combination of the adsorption of RuO_x clusters and the ultrasonic weltering in NaOH for 30 min was found to improve the capacitive performance of activated carbon. The composite composed of 10 wt.% RuO_x nanoparticles annealed in air at 200 °C for 2 h and 90 wt.% AC was found to show acceptable electrochemical characteristics for the application of electrochemical supercapacitors (i.e., the total specific capacitance of 111.7 F/g obtained at 25 mV/s, the potential window for charge–discharge from −0.2 to 0.9 V, and a fairly high-power property). The specific capacitance of RuO_x nanoparticles within these AC–RuO_x composites was promoted from 470 to 980 F/g by annealing in air at 200 °C for 2 h.

Acknowledgements

The financial support of this work, by the Industrial Technology Research Institute and the National Science Council of the Republic of China under contract no. NSC 91-2214-E-194-012, is gratefully acknowledged.

References

[1] B.E. Conway, Electrochemical Supercapacitors, Kluwer–Plenum Press, New York, 1999.
[2] A. Burke, J. Power Sources 91 (2000) 37.
[3] C.-C. Hu, Y.-H. Huang, J. Electrochem. Soc. 146 (1999) 2465.
[4] J.P. Zheng, J. Huang, T.R. Jow, J. Electrochem. Soc. 144 (1997) 2026.
[5] B.V. Tilak, C.-P. Chen, J. Electrochem. Soc. 143 (1996) 3791.
[6] J.P. Zheng, T.R. Jow, J. Electrochem. Soc. 142 (1995) L6.
[7] J.P. Zheng, P.J. Cygan, T.R. Jow, J. Electrochem. Soc. 142 (1995) 2699.
[8] C.-C. Hu, Y.-H. Huang, Electrochim. Acta 46 (2001) 3431.
[9] C. Lin, J.A. Ritter, B.N. Popov, J. Electrochem. Soc. 146 (1999) 3155.
[10] J.P. Zheng, Electrochem. Solid-State Lett. 2 (1999) 359.
[11] S.-L. Kuo, N.-L. Wu, Electrochem. Solid-State Lett. 6 (2003) A85.
[12] M. Ramani, B.S. Haran, R.E. White, B.N. Popov, L. Arsov, J. Electrochem. Soc. 148 (2001) A374.
[13] Y. Sato, K. Yomogida, T. Nanaumi, K. Kobayakawa, Y. Ohsawa, M. Kawai, Electrochem. Solid-State Lett. 3 (2000) 113.
[14] H. Kim, B.N. Popov, J. Power Sources 104 (2002) 52.
[15] C.-C. Hu, C.-C. Wang, Electrochem. Commun. 4 (2002) 554.
[16] C.-C. Wang, C.-C. Hu, Mater. Chem. Phys., submitted for publication.
[17] C.-C. Hu, K.-H. Chang, Electrochim. Acta 45 (2000) 2685.
[18] D.A. McKeown, P.L. Hagans, L.P.L. Carette, A.E. Russel, K.E. Swider, D.R. Rolison, J. Phys. Chem. B 103 (1999) 4825.
[19] C.-C. Hu, Y.-H. Huang, K.-H. Chang, J. Power Sources 108 (2002) 117.
[20] M. Pourbaix, Atlas of Electrochemical Equilibria in Aqueous Solutions, National Association of Corrosion Engineers, Houston, TX, USA, 1966.